Anal. Chem. **2004,** *76,* 7336−7345

Fluorescent Sensor for Imidazole Derivatives Based on Monomer−Dimer Equilibrium of a Zinc Porphyrin Complex in a Polymeric Film

Ying Zhang, RongHua Yang,* Feng Liu, and Ke′An Li

College of Chemistry and Molecular Engineering, Peking University, Beijing, 100871, China

A new zinc(II) porphyrin conjugate with an appended pyrene subunit has been synthesized and shown to exhibit significant and analytical usefulness for fluorescence sensing toward imidazole derivatives. The molecular recognition was based on the bridging interaction of the imidazole ring of analyte with the zinc(II) center of the porphyrin, while the transduction signal for the recognition process was the pyrene excimer fluorescence. The sensor was constructed and applied for fluorescence assay of histidine in aqueous solution by immobilizing the sensing material in a plasticized PVC membrane. When the membrane was bathed in an alkaline solution void of histidine, zinc(II) porphyrin was present in the monomer form, and pyrene emitted monomer fluorescence at 378 and 397 nm. With the presence of histidine in the sample solution, histidine was extracted into the membrane phase and bridged with the Zn(II) center of the porphyrin, causing the monomer porphyrin to be converted to its dimeric species. Since the formation of porphyrin dimer was accompanied by the enhancement of pyrene excimer emission at 454 nm, the chemical recognition process could be directly translated into a fluorescent signal. With the optode membrane M1 described, histidine in sample solution from 6.76×10^{-7} to 5.01×10^{-3} M can be determined. The limit of detection was 1.34×10^{-7} M. The optical selectivity coefficient obtained for histidine over biologically relevant amino acids and anions met the selectivity requirements for the determination of histidine in biological samples. Serum histidine values obtained by the optode membrane fell in the normal range of the content reported in the literature and were in good agreement with those obtained by HPLC.

The detection and identification of trace concentrations of biologically relevant compounds continue to be an important and active area of chemical and biomedical research.[1,2] Imidazoles are a common component of a large number of natural products and pharmacologically active molecules. The imidazole ring is present in the structure of some important biologically active compounds such as purine and histidine and functions as a ligand toward transition metal ions in a number of biologically important molecules.[3−5] Some of its derivatives and imidazole itself have also been used as corrosion inhibitors and adhesion promoters.[6,7] These facts make imidazole and its derivatives important target analytes. In the past years, several techniques have been described for the determination of imidazole derivatives, such as radioenzymatic, fluorometric, and electrochemical methods.[8−10] The most commonly used method for detection of an individual imidazole derivative in biological samples is chromatography, which is usually carried out through the combination of an effective separation technique such as thin-layer chromatography, gas chromatography, and HPLC and a derivation method, followed by UV−visible or fluorescence spectrometry.[11−13] High-performance capillary electrophoresis methods using derivation reagent have also been reported to improve selectivity.[14] But these methods are cumbersome, laborious, and most importantly, discontinuous and, thus, not amenable for real-time monitoring or on-site application.

To develop continuous assay methods for imidazole derivatives, ion-selective electrodes based on liquid- or solid-state membranes have been applied.[15−17] However, the instability of electrode potential and the use of a reference electrode limited their applications in remote monitoring or monitoring in vivo. Consequently, the development of new optical chemical sensors (op-

* To whom correspondence should be addressed. E-mail: Yangrh@pku.edu.cn. Fax: +86-10-62751708.

(1) *Chemical Sensors and Biosensors for Medical and Biological Applications*; Spichiger-Keller, U. E., Ed.; Wiley-VCH: Weinheim, 1998.
(2) *Fluorescent and Luminescent Probes for Biological Activity*, 2nd ed.; Mason, W. T., Ed.; Academic Press: New York, 1999.
(3) *Inorganic Chemistry-Principle of Structure and Reactivity* 3nd ed.; Huheeg, J. E., Ed.; Harper International: London, 1983.
(4) Mastuura, T.; Saito, I. *Tetrahedron* **1969**, *25*, 557−564.
(5) Sisko, J.; Kassick, A. J.; Mellinger, M.; Filan, J. J.; Allen, A.; Olsen, M. A. *J. Org. Chem.* **2000**, *65*, 1516−1524.
(6) Larsen, A. S.; Holbrey, J. D.; Tham, F. S.; Reed, C. A. *J. Am. Chem. Soc.* **2000**, *122*, 7264−7272.
(7) Micanovic, R.; Procyk, R.; Lin, W. H.; Matsueda, G. R. *J. Biol. Chem.* **1994**, *269*, 9190−9194.
(8) Shaff, R. E.; Beaven, M. A. *Anal. Biochem.* **1979**, *94*, 425−430.
(9) Li, X. H.; Ma, H. M.; Dong, S.; Duan, X. J.; Liang, S. C. *Talanta* **2004**, *62*, 367−371.
(10) Moreira, J. C.; Fogg, A. G. *Analyst* **1995**, *115*, 41−45.
(11) Leroy, P.; Nicolas, A.; Moreau, A. *J. Chromatogr.* **1983**, *282*, 561−569.
(12) Jensen, T. B.; Marely, P. D. *J. Chromatogr., B* **1995**, *670*, 199−207.
(13) Tateda, N.; Matsuhisa, K.; Hasebe, K.; Kitagima, N.; Miura, T. *J. Chromatogr., B* **1998**, *718*, 235−241.
(14) LaTorre, R. M.; Saurina, J.; Hernandez-Cassou, S. *J. Chromatogr. Sci.* **1999**, *37*, 353−359.
(15) Tastuma, T.; Watnable, T. *Anal. Chem.* **1992**, *64*, 143−147.
(16) Pihel, K.; Hsieh, S.; Jorgenson, J. W.; Wightman, M. R. *Anal. Chem.* **1995**, *67*, 4514−4521.
(17) Amini, M. K.; Shahrokhian, S.; Tangestaninejad, S. *Anal. Chem.* **1999**, *71*, 2502−2505.

10.1021/ac049477+ CCC: $27.50
Published on Web 11/17/2004

todes) in this field remains an important project of research, since the optodes can offer advantages that the analytical signal is free of influence of an electromagnetic field and easy to transmit over a long distance. In recent years, many effective optical chemical sensors for amines and amino acids have been successfully developed;[18−22] however, very few have been explored for imidazole derivatives. Notable exceptions include the work of Fabbrizzi and co-workers, who developed a competitive noncovalent fluorophore-displacement method that selectively responds to imidazole and histidine in aqueous solution.[23,24] Although the noncovalent assembly provides a simple block approach for chemosensing, the resulting ensemble may be less stable than a covalently linking sensory system.

The construction of a usefully covalent sensory molecule for an optical sensor is dependent on two general design features. One requirement is that a reversible recognition element be present to provide selectivity for a given analyte. The second general requirement is that the sensor must be able to exhibit a measurable response signal to the recognition process. The development of recognition sites in optical sensors has been vigorously pursued in the past decades. One of the most important of them that can be utilized in optical sensors involves the specific metal−ligand interactions of metalloporphyrins.[25−31] Recently, Meyerhoff and co-workers reported a novel optode toward chloride ion[30] and amine vapors[31] based on the dimer−monomer equilibrium reaction of indium(III) octaethylporphyrin in a polymeric film. The ligation of the analyte to the In(III) center, concomitantly breaks the equilibrium of the dimer and monomer of the porphyrin, yielding changes in the absorption spectra of the porphyrin. Indeed, it has been shown that in some cases, the Mn(III), Co(III), Sn(IV), and Ga(III) porphyrins also exist in monomer−dimer equilibrium interactions by hydroxide ion bridging.[32−36] These equilibrium interactions have been extensively applied in optical sensing toward anions and neutral molecules. It should be noted, however, that even though the number of such reports is large, the response signals of these sensors were confined to absorbance changes. While absorbance is sufficiently sensitive for many routine applications, it is not sensitive enough for microscopic measurements. The higher sensitivity of fluorescence over absorbance is established. Further, the use of fluorescence in an optical sensor provides a means to significantly reduce the required membrane volume while retaining the same signal-to-noise ratio, which in turn will shorten the response time. We are interested in developing new macrocyclic ligands as potential fluorescent sensors toward cationic ions[37,38] and neutral molecules.[22,39] Inspired by the success of the previous work of Meyerhoff et al., the goal of the present work is to extend the metalloporphyrin monomer−dimer equilibrium interaction to a novel fluorescent sensor.

There are numerous mechanisms by which fluorescent signal transduction may be affected. Recently, we reported a fluorescent sensor for silver ion based on an intramolecular exciplex formed in the monomer−dimer equilibrium system of the excited fluorophore, pyrene.[38] The large spectral shift for pyrene excimer versus monomer emission and high fluorescence quantum yields make such molecules attractive as fluorescence probes and chemosensors.[40−44] We report herein the first attempt to apply the pyrene excimer fluorescence emission in the metalloporphyrin monomer−dimer equilibrium reaction to signal the molecule recognition process fluorescently. Figure 1 shows the structure of the new design sensory molecule, Py-Zntpp. In alkaline solution, the ligand-free state of Py-Zntpp is present in its monomer species, and the fluorophore, pyrene, emits weak monomer fluorescence at 378 and 397 nm due to intramolecule photoinduced electron transfer (PET).[45] In the presence of a bridging ligand such as histidine, the ligation of the imidazole residue to the Zn(II) center of the porphyrin, causes the monomer species to be converted to dimer, yielding the strong excimer emission of pyrene at 454 nm with a little increase in the monomer fluorescence. The sensor was constructed and applied in the fluorescence assay of histidine in aqueous solution by immobilizing the sensing material in a plasticized poly(vinyl chloride) (PVC) membrane. The sensor was optimized and characterized with respect to response characteristics, membrane formulation, influence of pH, and the resultant amino acid selectivity.

(18) Kuroda, Y.; Kato, Y.; Hasegawa, J.; Kawanami, S.; Takahshi, M.; Shiraishi, N.; Tanabe, K.; Ogoshi, H. *J. Am. Chem. Soc.* **1995,** *117,* 10950−10958.
(19) Mizutani, T.; Wada, K.; Kitagawa, S. *J. Am. Chem. Soc.* **1999**, *121,* 11425−11431.
(20) Ait-Haddou, H.; Wiskur, S. L.; Lynch, V. M.; Anslyn, E. V. *J. Am. Chem. Soc.* **2001**, *123*, 11296−11297.
(21) Liu, R. P.; Regnier, F. E. *Anal. Chem.* **2003**, *75*, 4956−4963.
(22) Yang, R. H.; Wang, K. M.; Long, L. P.; Xiao, D.; Yang, X. H.; Tan, W. H. *Anal. Chem*. **2002**, *74*, 1088−1096.
(23) Fabbrizzi, L.; Francese, G.; Licchelli, M.; Perotti, A.; Taglietti, A. *Chem. Commun.* **1997**, 581−582.
(24) Hortalá, M. A.; Fabbrizzi, L.; Marcotte, N.; Stomeo, F.; Taglietti, A. *J. Am. Chem. Soc.* **2003**, *125*, 20−21.
(25) D'souza, F. *J. Am. Chem. Soc.* **1996**, *118*, 923−924.
(26) Barker, S. L. R.; Shortreed, M. R.; Kopelman, R. *Anal. Chem*. **1997**, *69*, 990−995.
(27) Badr, I. H. A.; Johnson, D.; Diaz, M.; Hawthorne, M. F.; Baches, L. G. *Anal. Chem*. **2000**, *72*, 4249−4254.
(28) Zhang X. B.; Guo, C. C.; Xu, J. B.; Shen, G. L.; Yu, R. Q. *Analyst* **2000**, *72*, 125, 867−870.
(29) Rakow, N. A.; Suslick, K. S. *Nature* **2000**, *406*, 710−713.
(30) Zhang, W.; Rozniecka, E.; Malinowska, E.; Parzuchowski, P.; Meyerhoff, M. E. *Anal. Chem*. **2002**, *74*, 4548−4557.
(31) Qin, W.; Parzuchowski, P.; Zhang, W.; Meyerhoff, M. E. *Anal. Chem*. **2003**, *75*, 332−340.
(32) More, W. E.; Seiler, K.; Lehmann, B.; Behring, C.; Hartman, K.; Simon, W. *Pure Appl. Chem*. **1989**, *61*, 1613−1619.
(33) Steinle, E. D.; Amemiya, S.; Buhlmann, P.; Meyerhoff, M. E. *Anal. Chem*. **2000**, *72*, 5766−5773.
(34) Cho, H. S.; Rhee, H.; Song, J. K.; Min, C. K.; Takase, M.; Aratani, N.; Cho, S.; Osuka, A.; Joo, T.; Kim, D. *J. Am. Chem. Soc.* **2003**, *125*, 5849−5860.
(35) Ikeda, C.; Tanaka, Y.; Fujihara, T.; Ishii, Y.; Ushiyama, T.; Yamamoto, K.; Yoshioka, N.; Inoue, H. *Inorg. Chem.* **2001**, *40*, 3395−3405.
(36) Hunter, C. A.; Sarson, L. D. *Angew. Chem., Int. Ed. Engl.* **1994**, *33*, 2313−2316.
(37) Yang, R. H.; Li, K. A.; Wang, K. M.; Liu, F.; Li, N.; Zhao, F. L. *Anal. Chem*. **2003**, *75*, 612−621.
(38) Yang, R. H.; Chan, W. H.; Lee, A. W. M.; Xia, P. F.; Zhang, H. K.; Li, K. A. *J. Am. Chem. Soc.* **2003**, *125*, 2884−2885.
(39) Yang, R. H.; Li, K. A.; Liu, F.; Li, N.; Zhao, F. L.; Chan, W. H. *Anal. Chem*. **2003**, *75*, 3908−3914.
(40) Yamauchi, A.; Hayashita, T.; Nishizawa, S.; Watanabe, M.; Teramae, N. *J. Am. Chem. Soc.* **1999**, *121*, 2319−2320.
(41) van der Veen, N. J.; Flink, S.; Deij, M. A.; Egberink, R. J. M.; van Veggel, F. C. J. M.; Reinhoudt, D. N. *J. Am. Chem. Soc.* **2000**, *122*, 6112−6113.
(42) Nishizawa, S.; Kato, Y.; Teramae, N. *J. Am. Chem. Soc.* **1999**, *121*, 9463−9464.
(43) Lewis, F. D.; Zhang, Y.; Letsinger, R. L. *J. Am. Chem. Soc.* **1997**, *119*, 5451−5452.
(44) Sahoo, D.; Narayanaswami, V.; Kay, C. M.; Ryan, R. O. *Biochemistry* **2000**, *39*, 6594−6601.
(45) Lin, Z. M.; Feng, W. Z.; Lueng, H. K. *J. Chem. Soc., Chem. Commun*. **1991**, 209−211.

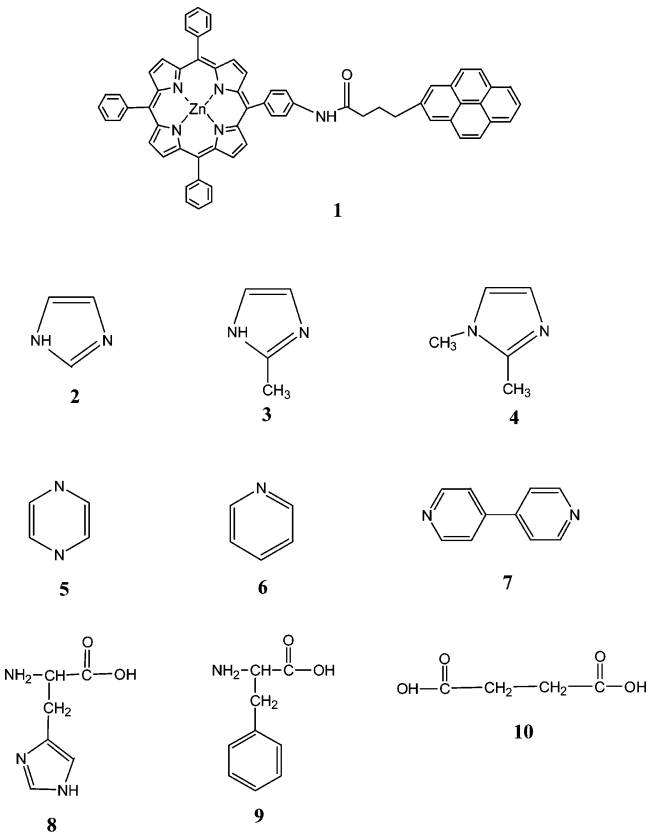

Figure 1. Structures of Py-Zntpp (**1**) and the ligands of imidazole (**2**), 2-methylimidazole (**3**), 1,2-dimethylimidazole (**4**), pyrazine (**5**), pyridine (**6**), bipyridine (**7**), histidine (**8**), phenylalanine (**9**), and butanedioic acid (**10**) examined in this work.

EXPERIMENTAL SECTION

Apparatus and Reagents. ^{1}HNMR spectra in $CDCl_3$ were measured with Invoa-400 (Invoa 400, 400 MHz) spectrometer with tetramethylsilane as internal standard. *J* values were given in hertz. Low-resolution mass spectra (MS) were obtained at 50−70 eV by fast atomic bombardment (FAB) on a Finnigan MAT SSQ-710 mass spectrometer. High-resolution MS were obtained on a Q-Star Pulsar I (Applied Biosystem/PE Sciex). UV−visible spectra were conducted on a Hitachi U-3010 UV−visible spectrophotometer. Fluorescence measurements were performed on a Hitachi F-4500 fluorescence spectrofluorometer. Data processing was performed on a Pentium IV computer with the software SigmaPlot. The pH of the test solutions were measured with a glass electrode connected to a PHS-3C pH meter (Shanghai, China) and adjusted if necessary.

All reagents were of analytical reagent grade. A stock solution of 0.05 M histidine (2-amino-3-(4-imidazolyl)propionic acid) was prepared by dissolving L-histidine in water. Solutions of 0.05 M interference amino acids or other ligands were prepared by dissolving the appropriate amount of each compound in water or ethanol−water. Working solutions were prepared by successive dilution of the stock solutions with 0.1 M Tris-HCl buffer (pH 9.0). For membrane preparation, PVC of high relative molecular weight, bis(2-ethylhexyl) sebacate (DOS), and tetrahydrofuran (THF) were purchased from Fluka AG and used as received. Unless otherwise stated, all solutions were prepared with redistilled water. Inorganic chemicals were of analytical-reagent grade and were used without purification or treatment.

Synthesis. The synthesis of the sensory molecule, Py-Zntpp, was accomplished by the route outlined in Scheme 1, where meso-tetraphenylporphyrin and 5-(4-nitrophenyl)-10,15,20-triphenylporphyrin were prepared and purified by literature procedures.[46,47]

5-(4-Aminophenyl)-10,15,20-triphenylporphyrin and 5-(4-Aminophenyl)-10,15,20 -triphenylporphinatozinc. 5-(4-Sminophenyl)-10,15,20-triphenylporphyrin was synthesized according to a modification of Kruper's procedure.[47] At room temperature, 5-(4-nitrophenyl)-10,15,20-triphenylporphyrin (3.9 g, 5.7 mmol) was dissolved in concentrated hydrochloride acid (60 mL) in a 500-mL beaker, followed by addition of excess of $SnCl_2 \cdot 2H_2O$ (2.8 g, 12.0 mmol). The resulting green mixture was quickly heated to 65−70 °C for 25 min and then cautiously neutralized with concentrated aqueous ammonia. Chloroform (100 mL) was added to the hot suspension, and the mixture stirred for 1 h. The $CHCl_3$ layer was separated, the aqueous layer was extracted 3 times with $CHCl_3$ (100 mL), and all $CHCl_3$ extracts were combined. The $CHCl_3$ solution was reduced to a smaller volume (~50 mL) on a rotary evaporator, washed first with dilute ammonia and then twice with water, dried over anhydrous sodium sulfate, and filtered. A 20-mL aliquot of ethanol−heptane (90:10, v/v) was added, and the mixture was slowly reduced in volume on a rotary evaporator to produce a very dark crystalline. The crude product was purified by column chromatography on silica gel eluted with $CHCl_3$ to give 5-(4-aminophenyl)-10,15,20-triphenylporphyrin as a purple material solid in 63% yield (2.4 g, 3.6 mmol). The amino porphyrin was directly added to a solution of $Zn(OAc)_2$ (0.8 g, 4.8 mmol) in methanol−$CHCl_3$ (20:80, v/v) and refluxed for 3 h. After that, 250 mL of water was added to the reaction mixture, and the organic layer was washed 3 times with water, dried over anhydrous magnesium sulfate, and filtered. The $CHCl_3$ solution was evaporated in vacuo using a rotary evaporator. The residue was purified by column chromatography on a silica gel column with $CHCl_3$−methanol (95:5, v/v) as eluent giving 5-(4-aminophenyl)-10,15,20-triphenylporphinatozinc in 84% yield (2.2 g, 3.01 mmol): ^{1}H NMR ($CDCl_3$, 400 MHz) δ 8.89 (d, 4H, J = 4.9 Hz, β-pyrrole), 8.85 (s, 4H, β-pyrrole), 8.24 (d, 6H, J = 7.4 Hz, *o*-phenyl), 8.03 (d, 2H, J = 7.8 Hz, aminophenyl), 7.79 (m, 9H, *m*/*p*-phenyl), 7.09 (d, 2H, J = 8.1 Hz, aminophenyl), 4.01 (s, 2H, NH_2); FAB-MS *m*/*z* 718 (M + 1).

Py-Zntpp.[48] Under a nitrogen atmosphere, to a solution of 5-(4-aminophenyl)-10,15,20 -triphenylporphinatozinc (0.72 g, 1.0 mmol) in anhydrous CH_2Cl_2 (50 mL) was added dropwise a mixture of 1-pyrenbutyryl chloride (0.46 g, 1.21 mmol), triethylamine (0.5 mL, 3.6 mmol), and anhydrous methanol (5 mL) at room temperature. The reaction mixture was stirred at room temperature for 24 h, after which saturated aqueous $NaHCO_3$ and CH_2Cl_2 were added. The organic layer was washed three times with water, dried over anhydrous magnesium sulfate, and filtered. The CH_2Cl_2 solution was reduced to a smaller volume on a rotary evaporator and purified by column chromatography on a silica gel column, and the column was eluted with CH_2Cl_2−petroleum ether (90:10, v/v) giving Py-Zntpp as a dark purple solid (0.54 g, 53%):^{1}H NMR ($CDCl_3$, 400 MHz) δ 11.20 (s, 1H, amide NH), 9.18 (2H, d, J =

(46) Adler, A. D.; Longo, F. R.; Finarelli, J. D. *J. Org. Chem.* **1967**, *32*, 476.
(47) Kruper, W. J., Jr.; Chamberlin, T. A.; Kochanny, M. *J. Org. Chem.* **1989**, *54*, 2753−2756.
(48) Lewis, F. D.; Zhang, Y. F.; Letsinger, R. L. *J. Org. Chem.* **1997**, *62*, 8565−8568.

Scheme 1. Reaction Scheme for Synthesis of Py-Zntpp

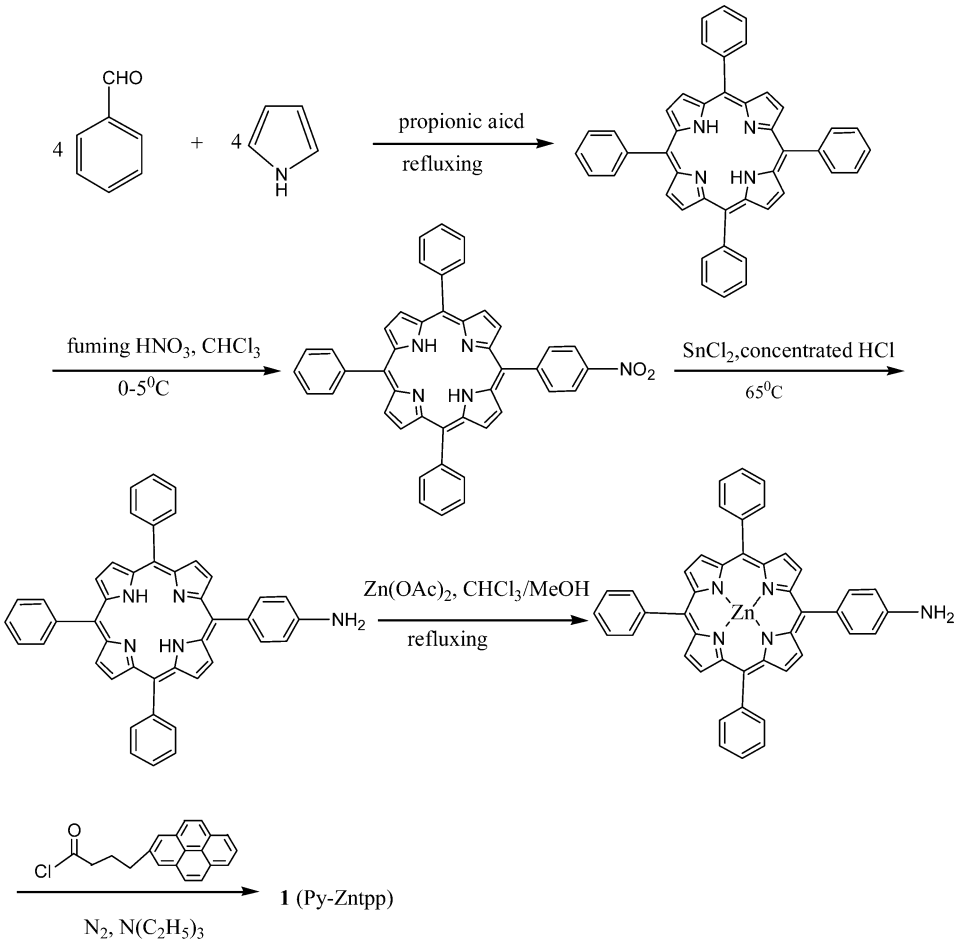

Table 1. Composition of Sensing Membrane Solution[a]

entry	Py-Zntpp (mg)	response slope ($-\partial\alpha/\partial c$, M^{-1})	dynamic range ($0.05 \le (1-\alpha) \le 0.95$, M)	detection limit ($(1-\alpha) = 0.01$), M)
M1	4.2	2.55×10^6	6.76×10^{-7}–5.01×10^{-3}	1.34×10^{-7}
M2	2.7	2.63×10^6	2.42×10^{-7}–6.31×10^{-4}	1.15×10^{-7}
M3	5.3	2.74×10^6	5.81×10^{-7}–6.37×10^{-4}	2.72×10^{-7}
M4	6.4	2.19×10^6	7.15×10^{-7}–1.13×10^{-3}	4.28×10^{-7}

[a] Each membrane contains 50 mg of PVC and 100 mg of DOS. Compositions of given amount were soaked up by microsyringes, mixed with 50 mg of PVC and 100 mg of DOS, and then diluted to 2 mL with fresh distilled THF.

4.8 Hz, β-pyrrole), 9.12 (d, 2H, J = 4.8 Hz, β-pyrrole), 9.04 (s, 4H, β-pyrrole), 8.46 (d, 2H, J = 8.4 Hz, phenyl bridge), 8.29–8.37 (m, 2H of phenyl bridge, 6H of *o*-phenyl), 7.96(d, 1H, J = 7.8 Hz, Py-H), 7.86 (s, 1H, Py-H), 7.74 (d, 1H, J = 7.8 Hz, Py-H), 7.67 (m, 9H, *m/p*-phenyl), 7.48 (d, 1H, J = 9.0 Hz, Py-H), 6.91 (d, 1H, J = 9.5 Hz, Py-H), 6.83 (d, 1H, J = 9.0 Hz, Py-H), 4.46 (d, 2H, J = 9.5 Hz, Py-H), 3.29 (m, 2H, J = 7.8 Hz, NHCO*CH*$_2$), 2.66 (dd, 1H, J = 8.5 Hz, Py-H), 2.36 (d, 2H, J = 7.3 Hz, Py-CH$_2$), 2.07 (s, 2H, J = 7.8 Hz, Py-CH$_2$*CH*$_2$); FAB-MS *m/z* 1065 (M + 1).

Membrane Fabrication. A membrane cocktail of M1 was obtained by dissolving 4.2 mg (0.8 μmol) of Py-Zntpp, 50 mg of PVC, and 100 mg of DOS in 2.0 mL of freshly distilled THF. An aliquot of 0.2 mL of this solution was applied to the surface of a circular 35-mm-diameter quartz plate, which was mounted on a rotating (rotating frequency 600 rpm) aluminum alloy rod under a THF-saturated atmosphere. After a spinning time of 5 s, a thin polymeric film was obtained onto the quartz plate. In a similar way, PVC membranes incorporating different amounts of Py-Zntpp were prepared from the described membrane cocktail (Table 1). The thicknesses of the resultant membranes were evaluated to be in the range of 3–5 μm, as measured by the interference pattern method.[49] When not in use, the optode membranes were stored in the dark.

Optical Measurements. The fluorescence and absorption titrations of Py-Zntpp with the analytes were carried out by adding a few microliters of a stock solution of the materials to 2.0 mL of 5.0×10^{-5} M methanol–water (60:40, v/v) of Py-Zntpp with a quartz cell (1.0×1.0 cm^2 cross section). The addition was limited to 50 μL so that the volume change was insignificant.

(49) Rosatzin, A.; Holy, P.; Seiler, K.; Rusterholz, B.; Simon, W. *Anal. Chem.* **1992**, *64*, 2029–2035.

To assess the fluorescence responses of the optode membrane M1 to histidine, experiments were carried out to monitor the fluorescence changes of the sensing membrane at 454 nm with an excitation wavelength of 347 nm. The quartz plate with a sensing membrane was fitted onto the front side of a flow cell. A 35-mm-diameter black PVC plate without sensing membrane was then fitted onto the other side to complete the cell. The cell was introduced in the fluorescence spectrophotometer at the appropriate position to guarantee the detection of fluorescence emission intensity without interference from the excitation source.[50] The limiting fluorescence intensities I_{min} and I_{max} of the optode membrane were detected in pH 9.0 blank solution and in 1.0×10^{-3} M histidine, respectively. After each measurement, the membrane was washed with Tris-HCl buffer solution until a stable fluorescence signal was observed before the next measurement. For the selectivity measurements, the separate solution method was used throughout by using solutions of corresponding amino acids or anions in Tris-HCl buffer solution.[51] The selectivity coefficients were evaluated by comparing the response function at $\alpha = 0.587$, which corresponds to 1.2×10^{-4} M histidine, the normal level in human serum.[52] The response to histidine was used as the standard.

Preparation of Human Serum Sample. For histidine determination, 1.0 mL of human serum was mixed with 1.0 mL of 5-sulfosalicylic acid (2%, w/v) in an Eppendorf polypropylene test tube for deproteinization. After shaking for 5 min, the homogenate was centrifuged (15 min, 100000 g) at 4 °C; the supernatant was then diluted 10-fold with buffer solution and stored at 4 °C for analytical determination.

The calibrators for serum measurement were prepared using buffer solution. These calibration solutions contained histidine at 5.0×10^{-6}, 2.5×10^{-5}, 1.0×10^{-4}, 2.5×10^{-4}, and 5.0×10^{-4} M, along with the typical coexisting components in human serum. The concentration of each component was chosen to match its normal level reported in human serum.[22]

RESULTS AND DISCUSSION

Design of the Sensory Molecule. The choice of the recognition element was guided by the considerations of the specific binding affinity with the imidazole residue and the formation of an ion-bridging system. In previous literature, it was demonstrated that zinc(II) porphyrin displays selective affinity toward imidazole derivatives via strong metal ion−nitrogenous base ligation interaction.[53−58] Further, the four-coordinated zinc porphyrin may accept one and only one axial ligand to form five-coordinated complex, since the electronic configuration is d,[10] and there are no empty d orbitals involved in the bonding.[53,54] Thus, the five-membered imidazole, which contains two nitrogen atoms in the one (N_1) and three (N_3) positions, can coordinate with two zinc centers to form a dimeric self-assembly of the porphyrin.[53−55,58] Although Cu(II),[59] Fe(II),[60] and Cd(II)[53] centers of porphyrins also appear to be excellent receptors for nitrogenous base, they cannot function as a fluorescent sensor, since these metal ions fully quench the pyrene fluorescence, and thus, monitoring the recognition process through the variation of fluorescence emission is prevented. Thus, we decided to use the zinc(II) porphyrin complex as a binding site.

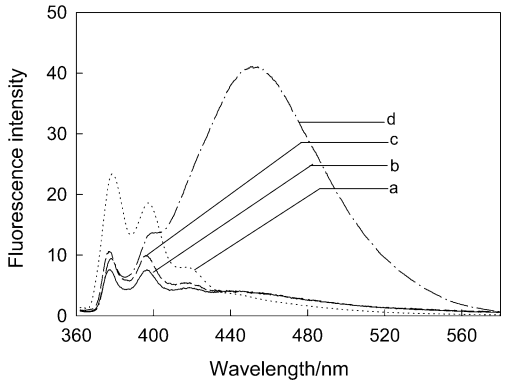

Figure 2. Fluorescence emission spectra of 1-methylpyrene (a) and Py-Zntpp (b) methanol−water, and the spectra of Py-Zntpp in the presence of 1,2-dimethylimidazole (c) and imidazole (d). Ligand concentration, 1.5×10^{-5} M; Py-Zntpp concentration, 5.0×10^{-5} M; excitation wavelength, 347 nm.

To signal the formation the porphyrin dimer fluorescently, we selected pyrene as the fluorescence reporting group. The fluorescence emission property of pyrene has been proven to be extremely sensitive to the polarity of the local environment. Formation of the dimeric self-assembled complex causes a remarkable change in fluorescence emission intensities of the pyrene excimer and monomer.[43,44] The structure of the sensory molecule, Py-Zntpp is shown in Figure 1, in which a zinc(II) porphyrin complex was linked covalently by an appended pyrene subunit via a propylene spacer. Py-Zntpp exhibits modest changes in the intensities of the monomer fluorescence emission and excimer fluorescence emission upon the Zn(II) center binding with an imidazole derivative.

Sensing of Py-Zntpp to Imidazole Derivatives in Solution. Figure 2 shows the fluorescence emission spectra of Py-Zntpp in methanol−water (60:40, v/v). Spectrum b was measured in the absence of imidazole derivatives, where Py-Zntpp shows a structured pyrene monomer emission band at 370−410 nm, almost coinciding in shape with that of 1-methylpyrene (spectrum a). However, the fluorescence intensity of Py-Zntpp is reduced to about one-fourth relative to that of 1-methylpyrene, indicating that the inner metalloporphyrin efficiently quenches the fluorescence of the inner pyrene moiety. This fluorescence quenching has been ascribed to the PET from the inner pyrene in singlet excited state to a low-spin Zn(II).[61] When an imidazole derivative was added to the solution of Py-Zntpp, appreciable increase in the monomer

(50) Yang, R. H.; Wang, K. M.; Xiao, D.; Yang, X. H.; Li, H. M. *Anal. Chim. Acta* **2000**, *404*, 205−211.
(51) Mohr, G. J.; Tirelli, N.; Spichiger, U. E. *Anal. Chem.* **1999**, *71*, 1534−1539.
(52) Pau, C. P.; Rechintz, G. A. *Anal. Chim. Acta* **1984**, *160*, 141−147.
(53) Miller, J. R.; Dorough, G. D. *J. Am. Chem. Soc.* **1952,** *74,* 3977−3981.
(54) Kirksey, C. H.; Hambright, P.; Storm, C. B. *Inorg. Chem.* **1969**, *8*, 2141−2144.
(55) Kirksey, C. H.; Hambright, P. *Inorg. Chem.* **1970**, *9*, 958−960.
(56) Kadish, K. M.; Shiue, L. R.; Rhodes, R. H.; Bottomleg, A. C. *Inorg. Chem.* **1981**, *20*, 1274−1279.
(57) Nappa, M.; Valentine, J. S. *J. Am. Chem. Soc.* **1978**, *100*, 5075−5080.
(58) Kuroda, Y.; Kawashima, A.; Hagashi, Y.; Ogoshi, H. *J. Am. Chem. Soc.* **1997**, *119*, 4929−4933.
(59) Baker, E. W.; Brokhart, V. G.; Corwin, A. H. *J. Am. Chem. Soc.* **1964**, *86*, 4587.
(60) Carver, G.; Tregenna-Piggott, P. L. W.; Barra, A.-L.; Neels, A.; Stride, J. A. *Inorg. Chem.* **2003**, *42*, 5771−5777.
(61) Heiler, D.; McLendon, G.; Rogalskyj, P. *J. Am. Chem. Soc.* **1987**, *109*, 604−607.

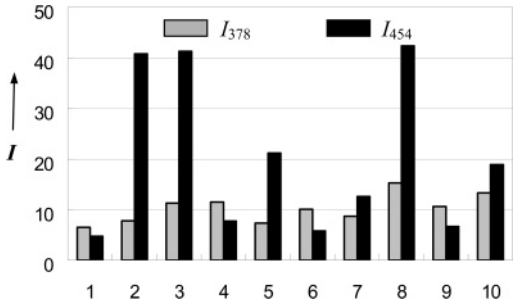

Figure 3. Monomer and excimer fluorescence intensity change profiles of Py-Zntpp in methanol−water in the presence of selected ligands: (1) no ligand, (2) imidazole, (3) 2-methylimidazole, (4) 1, 2-dimethylimidazole, (5) pyrazine, (6) pyridine, (7) bipyridine, (8) histidine, (9) phenylalanine, and (10) butanedioic acid. Ligand concentration, 1.5×10^{-5} M; Py-Zntpp concentration, 5.0×10^{-5} M; excitation at 347 nm, and emission monitored at 378 (gray) and 454 nm (black), respectively.

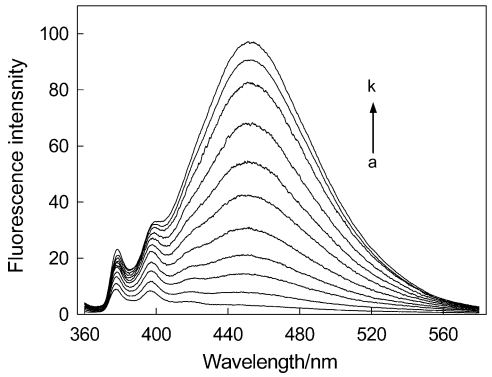

Figure 4. Fluorescence emission spectra of Py-Zntpp in methanol−water in the presence of varying concentrations of histidine: (a−k, respectively) 0, 7.5×10^{-7}, 1.5×10^{-6}, 2.5×10^{-6}, 5.0×10^{-6}, 1.5×10^{-5}, 2.5×10^{-5}, 5.0×10^{-5}, 1.5×10^{-4}, 2.5×10^{-4}, and 5.0×10^{-4} M). Py-Zntpp concentration, 5.0×10^{-5} M; excitation wavelength, 347 nm.

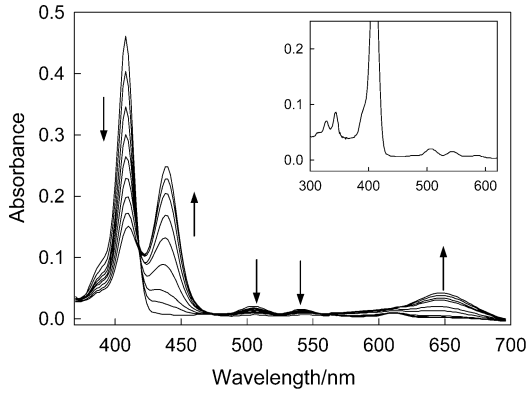

Figure 5. UV−visible spectral changes of Py-Zntpp (5.0×10^{-5} M) in methanol−water upon addition of histidine as host/guest molar ratio changes from 1:0 to 1:5. The arrows indicate the increases or decreases in the absorbance of the indicated band as increases in histidine concentrations. Inset: absorption spectrum of the ligand-free Py-Zntpp.

fluorescence emission at 378 and 398 nm was observed, as shown in spectrum c or d. These fluorescence enhancements are due to the ligation of the Zn(II) center with the nitrogenous base and the inhibition of PET quenching of the fluorophore by the metalloporphyrin.[62]

In addition to the increases in pyrene monomer fluorescence, Py-Zntpp also shows different excimer fluorescence response behaviors to imidazole derivatives with different structures. In the presence of imidazole, a structureless band with an emission maximum at 454 nm, typical of the pyrene excimer emission, appears as shown in spectrum d. However, Py-Zntpp does not exhibit significant excimer enhancement upon addition of 1,2-dimethylimidazole (spectrum c). The fluorescence intensity of Py-Zntpp at 454 nm is increased to 8.57-fold that of the original value by imidazole (1.5×10^{-5} M), while it is only 1.05-fold by 1,2-dimethylimidazole. Figure 3 shows the monomer and excimer fluorescence intensity changes of Py-Zntpp in the presence of imidazole derivatives and relative substrates. On the basis of the photospectroscopic data, it seems that histidine, 2-methylimidazole, pyrazine, butanedioic acid, and bipyridine behave like imidazole, which show, pyrene excimer fluorescence enhancement. The response sequence of Py-Zntpp for these ligands is imidazole ≈ 2-methylimidazole ≈ histidine > pyrazine > butanedioic acid > bipyridine. The small fluorescence response of Py-Zntpp to butanedioic acid may be due to weak affinity of the metal center to the carboxylate fragment, while that of bipyridine may be due to the steric effect. It should be noted that with titration of Py-Zntpp with the 1,2-dimethylimidazole, no significant excimer fluorescence response is observed, as those observed by pyridine and phenylalanine, confirming that signaling is promoted by Zn−Zn bridging of the im^- fragment.[24]

Figure 4 shows the typical response spectra of Py-Zntpp indicating the formation of porphyrin dimer with an increasing histidine concentration. Py-Zntpp exhibits significant changes in both the pyrene excimer and monomer fluorescence in the presence of different concentrations of histidine. The intensity of excimer emission increases considerably as an increase in histidine concentration, indicating formation of the intramolecular excimer of pyrene. Histidine also increases the pyrene monomer emission due to ligation with the metal center and inhibiting the PET quenching. However, the fluorescence response of Py-Zntpp to histidine at the 454-nm band is more sensitive than that at the 378-nm band. In our subsequent experiments, the optode membrane response toward histidine was made $\lambda_{ex} = 347$ nm and $\lambda_{em} = 454$ nm.

The sensing behavior of Py-Zntppto histidine can be more drastically demonstrated by virtue of the changes of the UV−visible spectra, and the results are shown in Figure 5. The maximums of the ligand-free state of Py-Zntpp in the Q-band region are at 504 and 546 nm, respectively, while the maximum of the Soret band occurs at 414 nm. These absorption bands are essentially identical to those observed for zinc meso-tetraphenylporphyrin. The additional bands at 330−370 nm are ascribed to the pyrene absorption bands (Figure 5, inset). The absorption spectrum of the Py-Zntpp molecule is essentially a superposition of the spectra of the porphyrin and pyrene chromophores and shows no significant perturbations indicating strong interaction between the linked moieties in ground state. In contrast, in the presence of histidine, a significant red-shift (28 nm) of the porphyrin Soret band absorption with the two Q-bands merging

(62) Lin, Z. M.; Feng, W. Z.; Lueng, H. K. *J. Chem. Soc., Chem. Commun.* **1991**, 209−211.

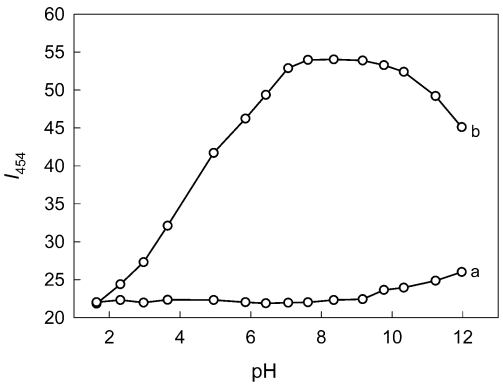

Figure 6. Effects of pH on the formation of metalloporphyrin dimer in the absence (a) or presence of histidine (b). Excitation was at 347 nm, and emission was monitored at 454 nm.

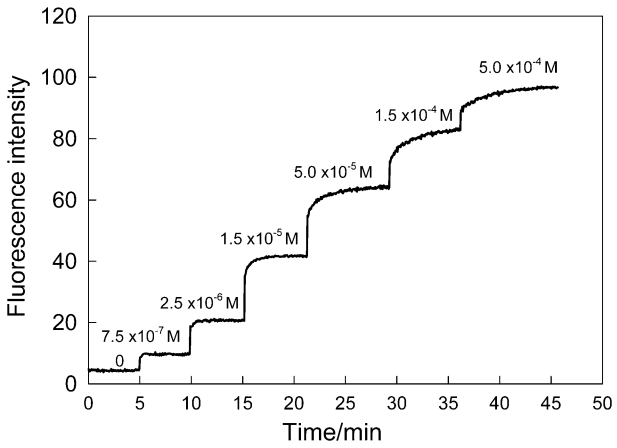

Figure 7. Time history of the optode membrane M1 responses to different concentrations of histidine. Fluorescence intensity was recorded at 454 nm with an excitation wavelength of 347 nm.

into a single peak at 646 nm is observed. The intensities of the Soret band and Q-bands gradually decrease, while those of the other two bands increase upon increasing histidine concentration, forming three clear isosbestic points. These spectral changes are characteristics for nitrogen base coordination with the Zn(II) center of the porphyrin.[58, 59]

Effect of pH on the Complex. To observe the effect of pH on the complex of Py-Zntpp with an imidazole derivative, a titration experiment was carried out in a spectrofluorometric cuvette, by adding standard NaOH to a solution containing 5.0×10^{-5} M Py-Zntpp, 2.5×10^{-5} M histidine, and excess of acid. The excimer fluorescence intensity of Py-Zntpp at 454 nm with the increase in pH is shown in Figure 6. It is observed that, in the absence of histidine (curve a), the excimer fluorescence emission of Py-Zntpp is not significantly pH dependent in acidic or weak alkaline medium; however, at high pH the metalloporphyrin can dimerize and thus produces the excimer fluorescence increases of pyrene. Curve b shows the pH dependence of the pyrene fluorescence emission in the presence of histidine. At pH <7.0, decrease of the excimer fluorescence response is observed, while in alkaline medium, the fluorescence response of Py-Zntpp to histidine is nearly independent of pH, and the response reaches a maximum value and remains constant between pH 7.5 and 10. The curve reporting the excimer fluorescence enhancement as a function of pH can be conveniently interpreted according to the ligation process. At acidic medium, the imidazole residue cannot undergo deprotonation and, thus, cannot bridge with the metal center. In the working pH range of 7.5−10.0, histidine exists mainly in the neutral form, which is subjected to forming the bridging complex with the metalloporphyrin and causing excimer fluorescence enhancement of pyrene. The observed decreasing response at pH >10 could be due to formation of a metalloporphyrin−OH complex[63] and, thus, reducing its complex with the imidazole residue. In subsequent experiments, a pH 9.0 buffer solution was selected as optimum.

Optode Membrane Response and Principle of Operation. From the aforementioned discussion, the fluorescence response of Py-Zntpp to histidine at 454 nm is more sensitive than that at 378 nm. Figure 7 shows the typical response of the optode membrane M1 to histidine, as obtained after equilibration with Tris-HCl buffer solutions containing different concentrations of histidine. The fluorescence intensity was recorded at 454 nm with an excitation wavelength of 347 nm. As expected from the original design, the values of the fluorescence intensity of the optode membrane increase considerably as the concentration of histidine increases. This illustrates that the optode membrane can be used for assay of histidine in aqueous sample solution.

The fluorescence response of the optode membrane to histidine is based on the fact that histidine was extracted from the aqueous sample solution into membrane phase, and then the imidazole residue of the histidine deprotonated and bridged to the Zn(II) centers with the proton expelling from the membrane phase to aqueous solution phase. The complex equilibrium and corresponding equilibrium constant, K, can be expressed by the following:

$$2\mathrm{MP}_{(\mathrm{mem})} + \mathrm{imH}_{(\mathrm{aq})} \overset{K}{\rightleftharpoons} \mathrm{im(MP)}_{2(\mathrm{mem})} + \mathrm{H}^{+}_{(\mathrm{aq})} \qquad (1)$$

$$K = \frac{[\mathrm{im(MP)}_2]_{(\mathrm{mem})}[\mathrm{H}^+]_{(\mathrm{aq})}}{[\mathrm{imH}]_{(\mathrm{aq})}[\mathrm{MP}]^2_{(\mathrm{mem})}} \qquad (2)$$

where MP and imH denote Py-Zntpp and an imidazole fragment of the analyte, respectively; the concentration terms refer to the concentration of each species in the polymeric membrane phase or in the aqueous sample solution.

The optode membrane response parameter, α, may be defined as the ratio of the concentration of the free-state Py-Zntpp, $[\mathrm{MP}]_{(\mathrm{mem})}$, to the initial concentration of Py-Zntpp in the membrane phase, $[\mathrm{MP}]_{\mathrm{T(mem)}}$,

$$\alpha = \frac{[\mathrm{MP}]_{(\mathrm{mem})}}{[\mathrm{MP}]_{(\mathrm{mem})} + [\mathrm{imMP}]_{(\mathrm{mem})}} = \frac{[\mathrm{MP}]_{(\mathrm{mem})}}{[\mathrm{MP}]_{\mathrm{T(mem)}}} \qquad (3)$$

According to the mass balance, and inserting eq 3 into eq 2 gives

$$[\mathrm{imH}]_{(\mathrm{aq})} = \frac{[\mathrm{H}^+]_{(\mathrm{aq})}}{2K[\mathrm{MP}]_{\mathrm{T(mem)}}} \frac{1-\alpha}{\alpha^2} \qquad (4)$$

(63) Chaniotakis, N. A.; Chasser, A. M.; Meyerhoff, M. E.; Groves, J. T. *Anal. Chem.* **1988**, *60*, 185−188.

The pH of the sample solution was fixed at 9.0 in the measuring procedure. If the K value and the initial concentration of Py-Zntpp in the membrane phase are assumed to be constant over the whole dynamic range, and if all constant values are summarized in K', then eq 5 can be derived from eq 4

$$[\mathrm{imH}]_{(\mathrm{aq})} = \frac{1}{K'} \frac{1-\alpha}{\alpha^2} \tag{5}$$

α can be experimentally determined by measuring the fluorescence intensity of the optode membrane at 454 nm

$$\frac{1-\alpha}{\alpha} = \frac{I - I_{\min}}{I_{\max} - I} \tag{6}$$

where I is the fluorescence intensity of the optode membrane at the given concentration of histidine, $I_{\min}$ is the fluorescence intensity when the membrane was exposed to buffer without any histidine, and $I_{\max}$ is the fluorescence intensity after the polymeric membrane was in equilibrium with a very high concentration of histidine.

Combining eqs 5 and 6, the dependence of fluorescence intensity of Py-Zntpp on the analyte concentration is taken, allowing determination of histidine concentration in aqueous solution by using this optode membrane. Because the activity coefficients of the neutral histidine in aqueous solution are not available,[64] the concentrations rather than the active molalities are used in eq 2 to calculate the combining equilibrium constant. Consequently, it is not possible to assess the absolute K' values. But it is possible to calculate the relative selectivities between the interfering amino acids by calculating the horizontal distance between the amino acid response curves for a given degree of reaction at $\alpha = 0.587$ denoted K'^{Opt}.

Optimization of Membrane Composition. As revealed by eq 5, the response of the optode membrane is dependent on its composition. To study the composition effect, membranes of M1−M4 of different formulations were fabricated (Table 1). The response slope ($-\partial\alpha/\partial C$, $\alpha = 0.5$), dynamic working range, and detection limit of the membrane may be modified by controlling the relative amount of Py-Zntpp in the membrane preparation as depicted in Table 1. The dynamic working range of the membrane increases with an increase in the amount of Py-Zntpp in the membrane phase. However, more sensing material does not produce a greater response slope. Taking the working range and the response sensitivity into account, the optimal Py-Zntpp immobilized amount was 4.2 mg (0.8 μmol), 2.71 wt % relative to the total amount of the membrane cocktail.

Changing the type of plasticizer is another way to alter sensor characteristics. Appropriate plasticizers must be selected to obtain a transparent and flexible membrane, which has the maximum response to the analyte. Sensing membranes made of different plasticizers were fabricated; membrane containing DOS gives the maximum sensitivity to histidine. The optimum ratio of DOS and PVC was 2:1 (w/w).

Characteristics of the Histidine Optode Membrane. With the optimum conditions, the theoretical prediction curve for M1 was constructed based on eqs 5 and 6. In Figure 8a, α is given as a function of the logarithm of histidine concentration at pH 9.0. The experimental data points were fitted to eqs 5 and 6 by adjusting K' value. The best curve fitting was obtained with $K' = 2.1 \times 10^7$ M^{-2}. The good correlation of the measured data with the theoretical predication confirms the validity of the assumption made in eq 1. The curve can serve as the calibration curve for the determination of histidine concentration. The dynamic working range covers from 6.76×10^{-7} to 5.01×10^{-3} M histidine referring to $0.05 \le (1-\alpha) \le 0.95$.[65] The limit of detection is 1.34×10^{-7} M referring to $(1-\alpha) = 0.01$.[65] The response sensitivity, defined as $-\partial\alpha/\partial C$ at $\alpha = 0.5$, is 2.25×10^6 M^{-1}.

The reproducibility and reversibility of the optode membrane were studied by alternatively recording the fluorescence intensity of the optode membrane exposed to different concentrations of histidine. Figure 9 shows the fluorescence response of M1 at $\lambda_{\mathrm{ex/em}} = 347/454$ nm versus time when the membrane was exposed to histidine buffer solution with repeated concentration step changes between 2.5×10^{-6} and 2.5×10^{-5} M histidine. The relative standard deviations of the fluorescence intensity for the two solutions were found to be 1.48 (2.5×10^{-6} M histidine, $n = 4$) and 1.96% (2.5×10^{-5} M histidine, $n = 5$), respectively. The results indicate that the membrane has good reproducibility and reversibility.

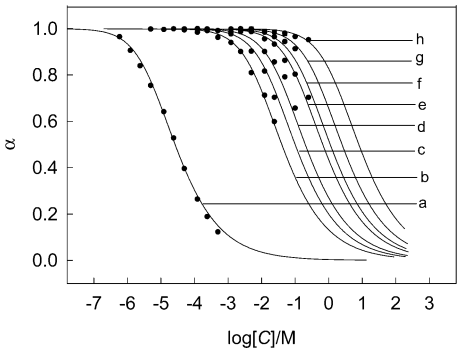

Figure 8. Responses of M1 to different amino acids: (a) histidine, (b) tryptophan, (c) glutamine, (d) leucine, (e) arginine, (f) tyrosine, (g) lysine, and (h) methionine. The horizontal distance at $\alpha = 0.587$ between the calibration curve for histidine and that for an interfering amino acid represents the respective selectivity coefficient (log K'^{Opt}). •, experimental data points.

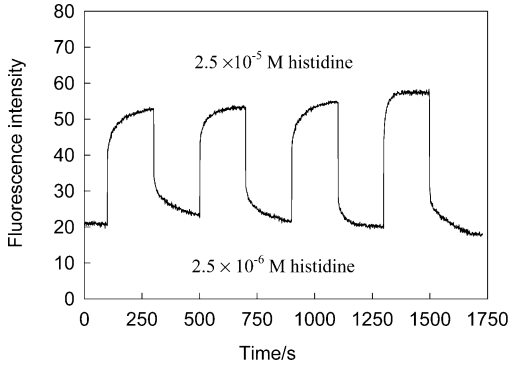

Figure 9. Reproducibility of the measurements obtained with optode membrane M1 by switching 2.5×10^{-6} and 2.5×10^{-5} M histidine. Fluorescence intensity was recorded at 454 nm with an excitation of 347 nm.

(64) Mohr, G. J.; Demuth, C.; Spichiger-Keller, U. E. *Anal. Chem.* **1998**, *70*, 3868−3873.

(65) Choi, M. M. F.; Wu, X. J.; Li, Y. R. *Anal. Chem.* **1999**, *71*, 1342−1349.

Table 2. Association Constants (K'^{M}) and Selectivity Coefficients (log K'^{Opt}) of the Optode Membrane M1 for Amino Acids and Common Anions in Comparison with Histidine

analyte	K'^{M}	log K'^{Opt}	analyte	K'^{M}	log K'^{Opt}
histidine	2.1×10^7		NCS^-	3.1×10^3	−4.61
tryptophan	1.0×10^5	−3.18	salicylate	7.1×10^3	−4.70
glutamine	4.0×10^4	−3.58	F^-	4.1×10^4	−4.88
leucine	2.1×10^4	−3.88	NO_2^-	6.6×10^3	−5.31
arginine	6.4×10^3	−4.40	$H_2PO_4^-$	4.3×10^4	−5.38
tyrosine	3.8×10^3	−4.70	Cl^-	9.4×10^3	−5.63
lysine	1.3×10^4	−5.06	SO_4^{2-}	1.6×10^3	−5.91
methionine	1.1×10^4	−5.54			

Table 3. Determinations and Recovery Tests of Histidine in Human Serum Sample[a]

histidine added (10^{-5} M)	histidine found by present method (10^{-5} M)	rec (%)	histidine found by HPLC (10^{-5} M)[b]
sample 1 + 0	11.31 ± 0.14		11.86 ± 0.26
sample 2 + 0	11.63 ± 0.13		11.47 ± 0.31
sample 3 + 0	10.97 ± 0.21		11.23 ± 0.17
sample 1 + 2.5	13.70 ± 0.25	95.6	
sample 1 + 5	16.57 ± 0.19	105.2	
sample 1 + 20	30.67 ± 0.46	96.8	
sample 1 + 50	60.62 ± 0.88	98.6	

[a] Average of three determinations. [b] The data were provided by "Analytical Center of Peking University".

The forward response time, t_{95} (time needed for 95% of the total signal change to occur), of the optode membrane is in the range of 3−5 min, whereas the reverse response time is in the range of 4−6 min (see Figure 9). Dynamic flow of the sample solution can shorten the response time. The changes of the membrane thickness in the range of 4 ± 0.2 μm cause no significant increase or decrease in response time. However, when the thickness of the membrane reaches the order of millimeters, no significant response is observed within 24 h. When the responses of the same membrane to the different step changes in histidine concentration are measured, there is ~30% difference in the response time and the time required to reach equilibrium increases with increasing histidine concentration (see Figure 7). The response time of such optode is mainly governed by the diffusion process in the bulk of the membrane. For the optode membrane with Py-Zntpp, the rate of complex formation and particularly the rate of complex dissociation might play an important role.

From the fluorescence signal values of 2.5×10^{-5} M histidine taken every 15 min over a period of 6 h, a mean fluorescence intensity value of 53.4 and a standard deviation of 0.93 were obtained. The stability of the sensor in a short time is reasonable. The fluorescence response value of the optode membrane decreased ~6% after continuous 100 measurements. Nevertheless, the lifetime of the optode membrane is acceptable for analytic application.

Selectivity. To further define the responses of the optode membrane M1 to other amino acids and anions, M1 was subjected to different concentrations of L-amino acids and biologically relevant anions, In Figure 8, the membrane responses, α, at pH 9.0 are plotted as functions of the concentration logarithms of all kinds of amino acids. The curve fittings for the experimental points were calculated from eqs 5 and 6 by assuming a 1:2 complex ratio. The relative selectivities (log K'^{Opt}) between histidine and the interfering amino acids and anions can be obtained by calculating the horizontal distance between the amino acid response curves (the anion response curves are not shown) for a given degree of reaction at $\alpha = 0.587$, which corresponds to 1.2×10^{-4} M histidine, the normal level in human serum.[52] The response to histidine was used as the standard. The results are summarized in Table 2. The log K'^{Opt} values follow the order, histidine ≫ tryptophan > glutamine > leucine > arginine > tyrosine > lysine > valine > glycine > methionine. The order of selectivity for the some common anions is as follows: histidine ≫ NCS^- > salicylate > F^- > NO_2^- > $H_2PO_4^-$ > Cl^- > SO_4^{2-}. Such large differences in the fluorescence response of Py-Zntpp to amino acids and anions make this sensor effectively useful for assaying histidine concentration where high concentrations of other amino acids and anions pertain. Although histamine is a potential bridging ligand for a Zn(II) center in regard to the imidazole ring structure of the molecule, the amount of histamine present in human serum is ~10 000-fold lower than that of histidine.[66] In reality, histamine would not significantly affect the measurement of histidine. The result is important and helpful in validation of the method to meet the selectivity requirements of a histidine assay in physiological fields.

Application. As an application of the present optode membrane to a biological sample, the quantitative determination of histidine in human serum was carried out. For serum sample measurements, calibrators and serum samples were alternately pumped into the flow cell and stopped in the cell for 5 min to reach full equilibrium with standard or sample. The fluorescence responses of the samples were compared to the calibration curve. As shown in Table 3, the determined mean values of histidine in human serum sample prepared as described in the Experimental Section correspond very well to the values that obtained by the HPLC method and fell in the normal range of the content reported in the literature. Further, the recoveries of the method were in the range of 95.6−105.2%, as given in Table 3, showing that the proposed sensor can be satisfactorily applied to the quantitative determination of histidine in human serum.

CONCLUSIONS

We have described a new fluorescent sensor toward an imidazole derivative based on the monomer−dimer equilibrium interaction of a zinc porphyrin complex. The recognition process can be signaled by pyrene excimer emission. This new sensing scheme demonstrates the feasibility of exploiting the metallporphyrin-based absorbance sensor into a fluorescence sensing model. Due to the specific bridging reaction between the metal center and the imidazole ring, the selectivity of the sensor for histidine is excellent over other biologically important amino acids and anions, which is shown to be adequate for reversible and

(66) Keyzer, J. J.; Wolthers, F. A. J.; Muskiet, H.; Breukelman, H. F.; Kauffman, D. K.; Vries, D. K. *Anal. Biochem.* **1984**, *139*, 474−481.

accurate sensing histidine levels in biological samples. Although demonstrated here for the detection of histidine, it is likely that other porphyrin monomer−dimer equilibrium systems could be employed in a fashion similar to construct fluorescence sensors for detecting other substrates by choosing porphyrins with appropriate metal ion centers. Efforts to extend this design principle for fluorescence detection of different analytes are currently underway in our laboratory, and the results will be reported in due course.

ACKNOWLEDGMENT

Financial support from the National Science Foundation of China (Grant 20475005) is gratefully acknowledgment.

Received for review April 6, 2004. Accepted October 4, 2004.

AC049477+